Structure of Isocitrate Dehydrogenase with Isocitrate, Nicotinamide Adenine Dinucleotide Phosphate, and Calcium at 2.5-Å Resolution: A Pseudo-Michaelis Ternary Complex†

Barry L. Stoddard,‡ Antony Dean,§ and Daniel E. Koshland, Jr.*

Department of Molecular and Cellular Biology, Division of Biochemistry, 229 Stanley Hall, University of California, Berkeley, California 94720

Received December 15, 1992; Revised Manuscript Received May 13, 1993®

ABSTRACT: The structure of isocitrate dehydrogenase (IDH) with a bound complex of isocitrate, $NADP^+$, and Ca^{2+} was solved at 2.5-Å resolution and compared by difference mapping against previously determined enzymatic complexes. Calcium replaces magnesium in the binding of metal–substrate chelate complex, resulting in a substantially reduced turnover rate. The structure shows the following: (i) A complete, structurally ordered ternary complex (enzyme, isocitrate, $NADP^+$, and Ca^{2+}) is observed in the active site, with the nicotinamide ring of $NADP^+$ exhibiting a specific salt bridge with isocitrate. The binding of the cofactor nicotinamide ring is dependent on this interaction. (ii) Isocitrate is bound by the enzyme with the same interactions as those found for the magnesium/substrate binary complex, but the entire molecule is shifted in the active site by approximately 1 Å in order to accommodate the larger metal species and to interact with the nicotinamide ring. The distances from isocitrate to the bound calcium are substantially longer than those previously found with magnesium. (iii) NADP in the *Escherichia coli* IDH has a novel binding site and conformation as compared to previously solved dehydrogenases. (iv) The orientation and interactions of the nicotinamide ring with the substrate are consistent with the stereospecificity of the enzyme-catalyzed reaction.

Isocitrate dehydrogenase (IDH) from *Escherichia coli* [*threo*-D-isocitrate:$NADP^+$ oxidoreductase (decarboxylating), EC 1.1.1.42] catalyzes the conversion of isocitrate to α-ketoglutarate and CO_2. The enzyme is dependent on NADP and on bound metal (usually Mg^{2+}) and lies at an important branch point in carbohydrate metabolism (Kornberg & Madsen, 1957). The enzyme is completely inactivated by phosphorylation of an active site serine residue (LaPorte & Koshland, 1982), and the effect of the phosphorylation can be largely duplicated by an aspartate from serine substitution, suggesting an important electrostatic effect (Thorsness & Koshland, 1987).

The structure of IDH, a dimer of 416 residues, has been previously been solved at 2.5-Å resolution as apoenzyme, as phosphorylated apoenzyme, as a binary complex of isocitrate and Mg^{2+}, and as a binary complex with $NADP^+$ in the absence of substrate and metal (Hurley *et al.*, 1989, 1990a,b, 1991). Isocitrate is bound in the active site primarily through interactions between its free carboxylate groups and several conserved basic residues and the metal ion (Hurley *et al.*, 1990b). Modeling of the binary complex of isocitrate and Mg^{2+} in the active site indicates that phosphorylation of serine 113 prevents substrate binding through direct electrostatic and steric interactions between the phosphate oxygens and the γ-carboxylate of isocitrate (Hurley *et al.*, 1990a). This has been confirmed kinetically using (2*R*)-malate, a substrate lacking the γ-carboxyl group (Dean & Koshland, 1990).

The crystal structure of IDH bound with $NADP^+$ in the absence of substrate provides ordered electron density only for the adenosyl portion of the cofactor (Hurley *et al.*, 1991). This observation is attributed to the absence of interactions between bound substrate, metal, and the nicotinamide ring which might be necessary in order to form a fully ordered complex with $NADP^+$. In order to determine the conformation of $NADP^+$ adopted by isocitrate dehydrogenase during turnover and to examine the interactions between substrate and cofactor which result in the enzyme's stereospecificity and kinetic mechanism, we have solved the structure of IDH with a bound ternary complex of isocitrate, $NADP^+$, and Ca^{2+}. Calcium has been shown to bind to the enzyme as a complex with isocitrate, to act as a competitive inhibitor of magnesium, and to cause almost complete inhibition of turnover as shown in Table I (Lee and Koshland, in preparation).

MATERIALS AND METHODS

Isocitrate dehydrogenase was purified (Reeves *et al.*, 1972; LaPorte *et al.*, 1985) and crystallized (Hurley *et al.*, 1989) as described previously. Protein at 60 mg/mL was diluted with double-distilled H_2O to a final concentration of 20 mg/mL. Hanging drop crystallizations were set up at room temperature by mixing 10 μL of the protein solution with 10 μL of unbuffered 40% saturated ammonium sulfate on a siliconized microscope cover slip. The drop then equilibrated against a 500-μL reservoir of the ammonium sulfate solution in a tissue culture plate well. Crystals grew within 2 weeks which were 0.7–1.0 mm per side, space group $P4_32_12$. The unit cell dimensions were refined to $a = b = 105.7$ Å, $c = 150.8$ Å during data processing.

The crystals were soaked with the three components of the slowly reactive ternary complex. Ten microliters of a 2× stock

† This work was supported by National Science Foundation Grant 04200 and by Materials Science Division, U.S. Department of Energy, under Contract No. DE-AC03-76SF00098. In addition, B.L.S. was supported by a postdoctoral fellowship from the Helen Hay Whitney Biomedical Sciences Foundation during all the work described in this manuscript.

‡ Present address: Division of Basic Sciences, Fred Hutchinson Cancer Research Center, 1124 Columbia St., Seattle, WA 98104.

§ Present address: Chicago Medical School, Green Bay Rd., North Chicago, IL.

® Abstract published in *Advance ACS Abstracts,* August 15, 1993.

0006-2960/93/0432-9310$04.00/0

Table I: Kinetic Effects of Calcium vs Magnesium in IDH Catalysis

metal	ionic radius (Å)	K_d (μM)	rates [nmol min^{-1} (mg of enzyme)$^{-1}$] forward	reverse
Mg^{2+}, pH 7	0.66	6	77 600	15 500
Ca^{2+}, pH 7	0.99	2	88	8
Ca^{2+} [pH 5.5, 40% satd $(NH_4)_2SO_4$]		<1	<0.1	

Table II: Data Processing and Refinement Statistics

crystal	1	2
exposure time (h)	5	4
rotations (deg)	30	22
radiation-induced decay (%)	24	17
total unique reflections	20 124	14 949
overlapping reflections	10 445	

Final Data Set and Refinement	overall	2.75–2.5 Å
R_{merge}[a] (%)	9.0	13.1
R_{symm}[b] (%)	8.6	12.4
total structure factors	24 628 (82%)	5125 (70%)
resolution (Å)	30–2.5	
refinement R-factor[c] (%)	19.5	27.0

Structural Statistics	
total atoms	3880
bond distance rms (Å)	0.017
bond angle rms (deg)	3.7
dihedral rms (deg)	24.3

[a] Overall R-factor (on intensities) between the same reflections from each crystal after scaling, correction for absorption and polarization. $R = \Sigma_j[I_1(j) - I_2(j)]/\Sigma_j[I(j)]$. [b] Initial overall R-factor (on intensities) between all symmetry-related reflections in the final merged data set.[c] $R = \Sigma_j|[F_{obs}(j) - F_{calc}(J)]|/\Sigma_j[F_{obs}(j)]$.

solution (50% saturated ammonium sulfate, 167 mM isocitrate and NADP, and 50 mM Ca^{2+}) was added directly to the equilibrated drop containing the crystals, and the soak proceeded overnight. The crystals were then mounted in quartz capillaries with mother liquor at either end of the capillary. The mount was sealed with mineral oil and paraffin wax.

Data were collected on an R-axis imaging plate area detector with a Rigaku RU-200 rotating-anode X-ray generator operating at 50 kV, 150 mA. The RAXIS data collection software package (Molecular Structure Corp.) was used to collect and process the data. Two crystals were used to collect a data set to 2.5-Å resolution using 1° rotations at 10 min/deg. A total of 24 628 reflections (82% of the unique data) were present in the final data set after a 2σ cutoff was applied. The overall R_{merge} between the two crystals was 9% on intensities and the overall R_{symm} was 8.6% (see Table II for data statistics). These values compare favorably with past reported IDH data sets (Hurley *et al.*, 1989, 1990a,b, 1991) and are indicative of the instability of the crystals in the X-ray beam.

Structural Refinement and Map Calculations. The data set was placed independently into both XPLOR simulated annealing refinement (Brunger *et al.*, 1987) and PROLSQ least-squares refinement (Konnert & Hendrickson, 1980) using the structure of uncomplexed isocitrate dehydrogenase (Hurley *et al.*, 1989) from the Brookhaven Protein Data Bank (Berstein *et al.*, 1977) as the initial model (Brookhaven no. 1ICD). No coordinates for substrate, cofactor, metal, or water molecules were included at any stage of these refinements. XPLOR refinement was performed against the data set from 8- to 2.5-Å resolution. We used a protocol in which the structure, after the initial static energy minimization, is heated to 4000 °C and then immediately placed into a slow cooling (50 ps) annealing minimization. No extended dynamics were performed during the heat stage of the refinement. Sequential cycles of least-squares refinement were run using the same initial model. In both refinements, the R-factor was 35% initially and 21.0% after convergence.

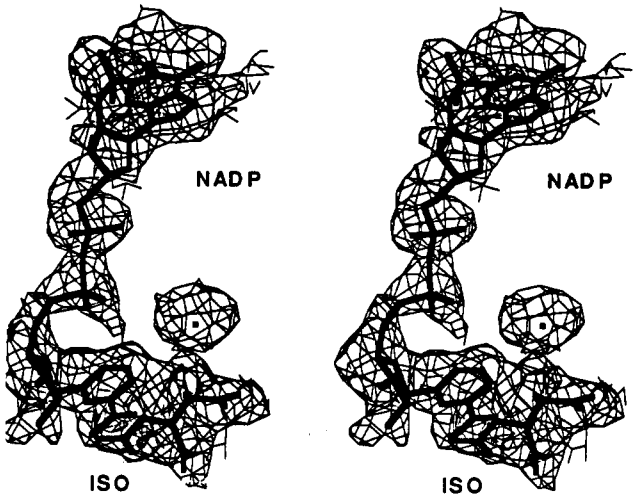

FIGURE 1: Electron density for the bound ternary complex as observed in an $F_o - F_c$ difference Fourier synthesis. The map was calculated after the initial round of annealing refinement with the protein coordinates only. No coordinates for the bound ternary complex were included in this refinement round or the ensuing phase calculation. The map is contoured at 2σ. The heavy atoms and bonds are shown for the members of the bound ternary complex (isocitrate, $NADP^+$, and Ca^{2+}).

[F_o (isocitrate, $NADP^+$, Ca^{2+}) – F_c (apoenzyme)] α_{calc} difference Fourier syntheses were then calculated using the protein coordinates from each refinement to supply phases. These maps were examined using the program FRODO (Jones, 1978) on an Evans and Sutherland PS300 graphics display. The largest features in these maps corresponded to the previously solved positions of bound metal, cofactor, and nucleotide, with additional density for fully ordered nicotinamide. The resulting maps agreed with one another both overall and in detail about the presence, position, and conformation of the bound complex. The three members of the ternary complex were manually built into the structure and the refinement was continued using XPLOR. No heating and annealing was performed in the second round of refinement. The final structure had an R-factor of 19.5% and a bond distance rms of 0.017 Å from ideality. The occupancy of the bound substrate, metal, and cofactor were fixed at unity during the refinement, and their individual atomic temperature factors were allowed to refine independently. The values of these B-factors ranged from 20 to 30 Å^2 and are comparable to the surrounding protein side chains in the active site, indicating that the assignment of the bound ternary complex is correct. The results of the final refinement are shown in Table II.

RESULTS

The electron density for bound cofactor, substrate, and calcium is well formed and can be modeled by NADP and isocitrate through simple adjustments in torsion angles through the pyrophosphate backbone and by a change in the nicotinamide sugar pucker (Figure 1). The conformation of the ribose rings is inferred from the orientation of the nicotinamide ring relative to the phosphate backbone of the cofactor. The

Table III: Distances and Geometries for Representative NAD(P) Structures[a]

enzyme[b]	stereo	metal	adenine ribose pucker[c]	nicotinamide ribose pucker[c]	ring–ring distance (Å)	ring–ring angle (deg)	Ca–C4 distance (Å)	N–C4–Ca angle (deg)
NAD (free acid)			C2′	C2′	9.6	14		
NAD (lithium salt)			C2′	C3′	11	113		
LDH	A	none	C3′	C2′	14.8	47	2.3	147
MDH	A	none	C3′	C2′	14.3	80	3.8	112
GAPDH (red)	B	none	C2′	C3′	15	73		
GAPDH (green)	B	none	C3′	C2′	15	82		
LADH	A	Zn	C3′	C3′	14	80	3.9	101
IDH	A	(Ca)	C2′	C4′	14	61	3.5	114

[a] The substrates or analogues used to measure distances and angles from "Ca" to C4 of the nicotinamide ring in the ternary complexes were isocitrate (IDH), DMSO (LADH), sulfate (MDH), and the covalent cofactor–substrate analogue S-lac-NAD (LDH). For GAPDH only the positions of inorganic phosphate in the absence of substrate have been determined in complex with enzyme and cofactor, and therefore no distances or angles to the substrate Ca have been estimated. [b] LDH, lactate dehydrogenase; MDH, malate dehydrogenase; GAPDH, glyceraldehyde-3-phosphate dehydrogenase; LADH, horse liver alcohol dehydrogenase; IDH, isocitrate dehydrogenase. [c] All sugar puckers presented are endo in both the adenosyl and nicotinamide ribose sugars.

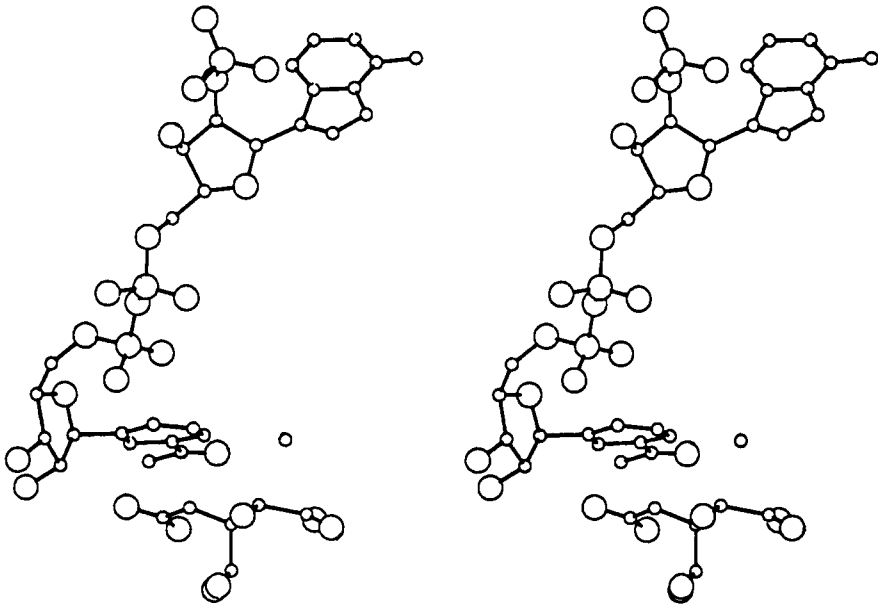

FIGURE 2: Interactions between bound isocitrate, Ca^{2+}, and the $NADP^+$ cofactor. The primary binding interaction to the nicotinamide moiety is a polar interaction with the bound isocitrate molecule. A specific electrostatic interaction is observed between the γ-carboxyl of the substrate and the nicotinamide ring nitrogen (N1); this interaction may reflect the formation of a nonproductive complex in the presence of Ca^{2+}. The distance between C2 of isocitrate and C4 of the nicotinamide (the atoms participating in hydride transfer) is 3.5 Å.

crystallographic electron density for the adenosyl portion of the cofactor and for the bound isocitrate molecule agrees with that for previously solved binary complexes of IDH (Hurley *et al.*, 1990b, 1991). The resulting complex between substrate and nicotinamide ring provides distances and angles for hydride transfer which are consistent with previously solved structures of dehydrogenases in complex with cofactor and substrate analogues (Table III). The peak corresponding to the bound calcium ion exhibits bond lengths to isocitrate which are significantly longer than those observed for magnesium in IDH. This may be related to the nonproductive kinetics of calcium in the enzyme, for which V_{max}/K_m is decreased by about 10^5 compared to turnover in the presence of magnesium, as shown in Table I.

The position of the bound adenosyl ring of $NADP^+$ corresponds to the position previously observed in the absence of substrate and metal (Hurley *et al.*, 1991). At the other end of the cofactor, the nicotinamide ring is closely associated with isocitrate through its *re* face (Figure 2). A distance of 3.5 Å exists between the C2 carbon of the substrate (the hydride donor) to C4 of the nicotinamide ring (the hydride acceptor). The angle through the nicotinamide ring to the substrate hydride donor carbon is 114°. This distance and angle is consistent with other previously solved dehydrogenase ternary complexes (Table III), which range from 2.3 to 3.9 Å and 101° to 147°, respectively.

Isocitrate moves by approximately 1 Å away from Tyr 160 and toward the nicotinamide ring as compared to the binary complex of isocitrate and Mg^{2+}. This motion is caused by a combination of the presence of the calcium ion (rather than magnesium) and the interaction between the negatively charged isocitrate and the positively charged nicotinamide ring and is the only significant conformational difference between the structure reported here (a ternary complex of substrate, cofactor, and Ca^{2+}) and the previously published binary complex (isocitrate and Mg^{2+}; Hurley *et al*, 1990b). This motion occurs primarily as a rigid body, with the contacts between protein side chains and the carboxylates of isocitrate maintained in the ternary complex. A rotation of the bond between C4 and C5 of isocitrate by approximately 45° allows the γ-carboxyl of the substrate to avoid a steric overlap with the nicotinamide ring, while maintaining the hydrogen bond to the γ-oxygen of serine 113 and forming a new bond to the nitrogen of the nicotinamide ring.

The $NADP^+$ cofactor is bound in an extended conformation with a distance of 14 Å between the center of the adenosyl

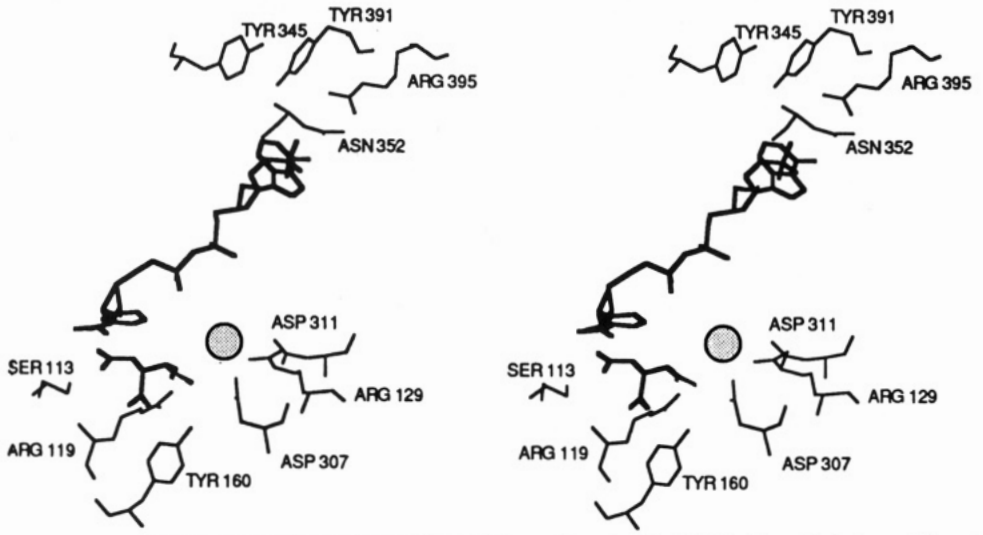

FIGURE 3: Stereo diagram of the active-site-bound ternary complex and the residues involved in binding substrate, metal, and cofactor. Residues from monomer 1 within 3.5 Å of the members of the bound complex are shown. $NADP^+$ is bound primarily through interactions with the adenine nucleotide [as previously described by Hurley *et al.* (1991)] and by interactions between isocitrate and the nicotinamide ring.

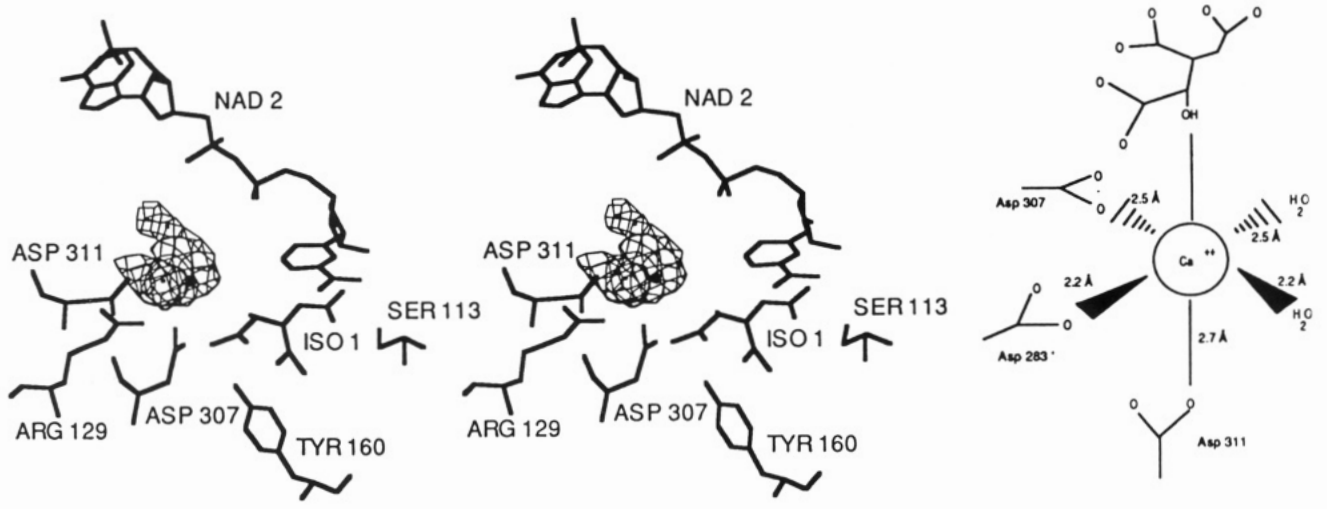

FIGURE 4: Stereo diagram of the bound ternary isocitrate/Ca^{2+}/NADP complex and residues and water molecules involved in binding the metal ion. Electron density is an $F_o - F_c$ Fourier synthesis after inclusion of isocitrate (without complexed metal) and NADP in the refinement and calculation of F_c's and phases. The calcium displays octahedral coordination, with bond distances of 2.2–2.7 Å, with the exception of the longer distance between calcium and the hydroxyl group of isocitrate (3.0 Å). The observed coordination of the calcium ion is represented schematically to the right of the stereo pair.

and nicotinamide rings. The phosphate backbone passes approximately 5 Å from the bound metal and leads into well-ordered density for the ribose and nicotinamide rings. The nicotinamide ring is in close proximity to the bound isocitrate and points back toward the cofactor phosphate backbone, and it appears to interact with the isocitrate molecule through polar interactions between the γ-carboxyl of isocitrate and the nicotinamide ring nitrogen and amide group. On the basis of this structure it is reasonable to assume that bound substrate is necessary in order to promote binding of the nicotinamide ring. The interactions observed between protein, substrate, and cofactor are shown in Figures 3 and 4.

The center of the bound Ca^{2+} is located approximately 1 Å from the previously solved position of Mg^{2+}. This movement, combined with the movement of isocitrate toward the nicotinamide ring, results in an increase in the distance between the metal and the oxygens of isocitrate by 0.6 Å, to 3.0 Å from the original 2.4 Å in the structure of the Mg^{2+}/isocitrate complex. Compared to the bond distances observed for calcium in several other calcium-binding protein structures such as calmodulin and troponin C and to the distance between isocitrate and Mg^{2+} in the enzymatic binary complex, the contact between isocitrate and calcium is unusually long and may effectively place the calcium beyond the proper contact distance necessary for strong chelation of isocitrate and stabilization of the enolate transition state (see Discussion). The Ca^{2+} ion is coordinated to the surrounding protein side chains in a similar manner to the related transition metal magnesium. Two water molecules (which are observed in difference maps) are involved in the metal coordination, and the metal is further coordinated by the isocitrate molecule and carboxylate oxygens of aspartate 307, 311, and 283′ (Figures 3 and 4).

DISCUSSION

Based on the results of previous crystallographic studies of IDH and a variety of active-site complexes (Hurley *et al.*, 1989, 1990a,b, 1991), an intriguing mechanistic question exists with regard to binding and catalysis by the enzyme. Modeling of possible conformations of $NADP^+$ in these structures correctly indicates that the isocitrate molecule should be buried in the active-site cleft by the nicotinamide ring during turnover,

which would argue in favor of an ordered, sequential binding mechanism in which isocitrate binds first, followed by $NADP^+$. This mechanism is in apparent contradiction with recent kinetic results from our laboratory indicating *random* binding of substrate and cofactor (Dean & Koshland, 1990). However, observation of the interaction between substrate and cofactor in the current structure of IDH complexed with bound isocitrate and $NADP^+$, combined with the previous observation that the nicotinamide ring of $NADP^+$ is disordered in the absence of substrate (Hurley *et al.*, 1991), appears to provide an excellent explanation of these results and reveals a strong consistency of kinetic, mutational, and crystallographic data as described below.

Kinetic and Stereochemical Mechanism of IDH. In the structure reported here, the phosphate backbone and nicotinamide portion of the cofactor are stabilized by electrostatic attractions to the charged isocitrate/metal complex. The nicotinamide ring (positively charged prior to hydride transfer) stacks on top of the isocitrate carboxyl groups, and the phosphate backbone of the cofactor passes approximately 5 Å from the cationic metal species. In the absence of substrate and metal, the possible interactions between nicotinamide and enzyme appear to be few, and the majority of the cofactor is exposed to solvent. Therefore, even though in the full ternary complex in the enzyme active site the isocitrate molecule is buried beneath the nicotinamide ring, a random binding mechanism is still allowed because of the fact that the phosphate backbone and nicotinamide ring are not bound and structurally ordered until isocitrate and metal are present in their binding sites.

Kinetic studies of IDH (Dean & Koshland, 1993) performed with wild-type and two mutant forms of the enzyme indicate that the wild-type dehydrogenase displays a steady-state random mechanism for the oxidative decarboxylation of isocitrate, with catalysis more rapid than product release. Those studies also indicate that the binding of each substrate (isocitrate or $NADP^+$) does not markedly influence the binding of the other, so that K_m for isocitrate to the enzyme is similar to the K_m for isocitrate to the E–$NADP^+$ complex. The random binding mechanism was also supported by initial rate, product inhibition, and dead-end inhibition studies. The structural observations reported in this work, in addition to previously reported structures of complexed IDH, support and explain these kinetic results at the molecular level: (i) Isocitrate and metal bind in the absence of $NADP^+$. (ii) $NADP^+$ binds in the absence of isocitrate, but it does so by affinity of its adenine moiety to produce a disordered complex which then allows isocitrate binding, producing a fully ordered Michaelis complex with the NADP. In the ternary complex the nicotinamide ring is properly positioned for hydride transfer primarily by interactions with substrate and metal. (iii) Both the bound substrate molecule and the phosphorylation site (Ser 113) are shielded from the solvent by the bulk of the bound nicotinamide ring. (iv) The kinetic mechanism for IDH and the structural pattern of binding agree with the observation that phosphorylation of the enzyme affects turnover primarily by preventing binding of isocitrate and by interfering with the proper orientation of the nicotinamide ring for hydride transfer. It also agrees with results of mutagenesis of the phosphorylation site; alteration of Ser 113 typically breaks a hydrogen bond to the γ-carboxyl of isocitrate and disrupts binding by steric hindrance, with an increase in the apparent K_m toward isocitrate and a reduction in V_{max}. In addition, an introduction of side chains in the region normally occupied by the γ-carboxyl of isocitrate and the side chain of Ser 113 increases the Michaelis constant of $NADP^+$. On the basis of this structure, this effect would appear to be explained by the interaction observed between the γ-carboxyl of isocitrate and both serine 113 and the ring nitrogen of the nicotinamide ring, a three-way interaction which is probably important for positioning the rigid nicotinamide ring for proper stereochemical transfer of a hydride from C2 of substrate to C4 of the cofactor. On the basis of this ternary complex structure, the proper positioning of the nicotinamide ring is directed primarily by the carboxylate groups of the substrate and serine 113.

The net structural result of these interactions in the active site is that the nicotinamide ring is closely associated with isocitrate through its *re* face (Figure 2). The β-carboxyl of isocitrate is anti to the hydride at the substrate C2, a configuration which is essential to the mechanism of hydride transfer. A distance of 3.5 Å exists between the C2 carbon of the substrate (the hydride donor) and C4 of the nicotinamide ring (the hydride acceptor). The angle through the nicotinamide ring to the substrate hydride donor carbon is 114°. This distance and angle are consistent with other previously solved dehydrogenase ternary complexes (Table III), which range from 2.3 to 3.9 Å and 101° to 147°, respectively. Upon hydride transfer, the isocitrate C2 becomes coplanar with C1, C3, and O2, thus narrowing the C2–C3–β-carboxyl bond angle and facilitating decarboxylation. The identity of the residues involved in proton abstraction from the 2-hydroxyl of isocitrate during hydride transfer and subsequent donation of a proton to C3 after decarboxylation are still ambiguous. The residues which are in close enough proximity to carry out this function are Lys 230′, Tyr 160, and any one of three arginines (119, 129, and 153). Identification of the actual residues involved in acid–base catalysis awaits further kinetic studies and time-resolved crystallographic experiments.

Dehydrogenases have traditionally been classified on the basis of their stereospecificity, according to which face of the nicotinamide ring serves as the site of hydride transfer. Transfer can occur either on the *re* face of the ring (leading to the designation of the enzyme as an A-type dehydrogenase) or to the *syn* face (a B-type dehydrogenase). IDH from *E. coli* has previously been classified as an A-type dehydrogenase (Hurley *et al.*, 1991), a designation which is supported by the structure of IDH in a ternary complex with isocitrate and cofactor. The nicotinamide ring of NADP in IDH appears to be preferentially stabilized in an A alignment relative to the isocitrate substrate through interactions between the nicotinamide ring, isocitrate, and the protein. In addition, the formation of electrostatic interaction between the isocitrate γ-carboxyl and the positively charged nicotinamide nitrogen may also promote the interaction of the nicotinamide amide with Asn 115, further enhancing the enzyme's stereochemical preference. In other previously solved structures of dehydrogenase structures, such as alcohol dehydrogenase (ADH), lactate dehydrogenase (LDH), and glyceraldehyde phosphate dehydrogenase (GAPDH), the nicotinamide ring is also preferentially stabilized in a single stereochemical orientation through interactions between the amide group and the neighboring protein. In the case of GAPDH, this residue is also an asparagine.

Conformation of $NADP^+$ and Differences from the Rossmann Fold. The coenzymes NAD and NADP, along with flavin adenine dinucleotide, are responsible for most enzyme-catalyzed dehydrogenation reactions. In all NAD(P)-dependent enzymatic redox systems categorized to date, the reactive site of the cofactor is at C4 of the nicotinamide ring,

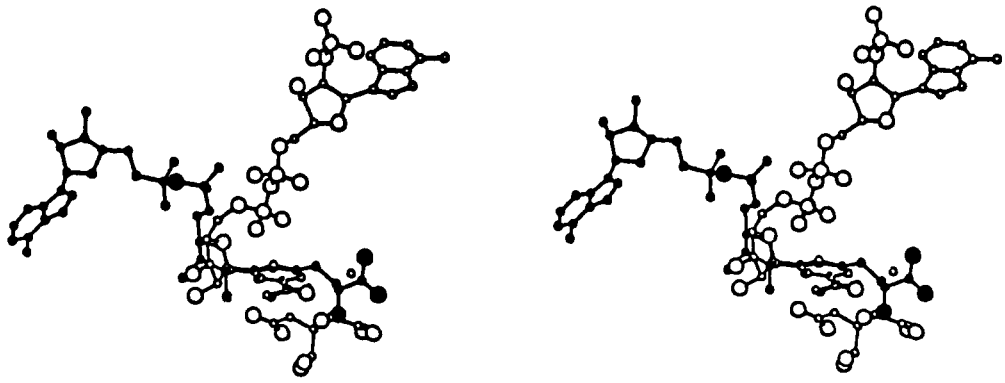

FIGURE 5: Superposition of NAD from lactate dehydrogenase (dark spheres; Brookhaven no. 5LDH) vs NADP from isocitrate decarboxylating dehydrogenase (open spheres). The cofactors in their complexes are superimposed at the nicotinamide and ribose rings. The adenosyl moiety from LDH curves to the left, and that from IDH curves to the upper right.

and the 1,4-dihydronicotinamide is the isomer formed after oxidation of substrate. Crystallographic structures of a number of dehydrogenases with bound, fully ordered NAD or a nicotinamide analogue have been solved at high resolution (Table III), including horse liver alcohol dehydrogenase (Eklund *et al.*, 1981, 1984), malate dehydrogenase (Birktoft *et al.*, 1989), lactate dehydrogenase (Grau *et al.*, 1981), and glyceraldehyde-3-phosphate dehydrogenase (Moras *et al.*, 1975). Each of these enzymes contain a single nucleotide binding domain per subunit which consists of a six-stranded parallel β-sheet. The NAD moiety is bound in a characteristic, extended conformation with the adenine and nicotinamide rings about 15 Å apart and their planes almost perpendicular to one another, as opposed to the more tightly folded conformation observed for unbound NAD^+ in the free acid and lithium salt forms, with a distance of about 10 Å between rings (Parthsarathy & Fridey, 1984). The ribose rings of the bound cofactors all have been observed to display a C2′ or C3′ endo pucker. The two mononucleotide rings are each associated with a binding site at the N-termini of three parallel strands of β-sheet, a structural unit commonly referred to as a Rossmann fold are usually conserved: a glycine at the end of the first β-strand, which accommodates the ribosyl moiety, and aspartate at the end of the second strand, which binds the O2′ of the ribose. The pyrophosphate backbone generally interacts with a number of basic residues and backbone amides, which help to produce an ordered bound structure.

IDH, however, displays a binding motif which is strikingly different from the typical Rossmann fold dehydrogenase (Table III). The enzyme consists of two domains, the smaller of which mimics the fold of LDH. The adenine-ribosyl moiety, however, binds at the interdomain cleft and is associated with two strands of antiparallel β-sheet. There is no clear interaction between enzyme and the hydroxyl of the adenine ribose, and the 2′-phosphate interacts with two arginines (292′ and 395) and two tyrosines (345 and 391). Additionally, in IDH the adenine ribose and pyrophosphate backbone are weakly bound and largely solvent-exposed. Although the cofactor displays a much different conformation than that of the previously solved Rossmann-fold dehydrogenases such as lactate dehydrogenase (Figure 5), the distance between the nicotinamide and adenine rings is approximately 14 Å, close to the distance observed for LDH. The differences in the conformation of the nicotinamide groups appear to be most evident in differences in the dihedral bond angles in the backbone phosphate groups and through the C4′ endo pucker of the nicotinamide ribose in IDH. NMR data has indicated that other dehydrogenases such as sorbitol dehydrogenase (nicotinamide ribose C1′ exo) also possess unique sugar conformations (Gronenborg *et al.*, 1984; Parthasarathy & Fridey, 1984). Thus it appears that certain bacterial dehydrogenases such as IDH (and the homologous enzyme isopropylmalate dehydrogenase) have evolved separately from previously studied dehydrogenases. This structural motif may be related to the decarboxylating function of the enzyme. The nucleotide binding sites of medium-chain acyl-CoA dehydrogenase (Kim & Wu, 1988), 6-phosphogluconate dehydrogenase (Adams *et al.*, 1986), and most recently the α-β barrel aldose reductase (Rondeau *et al.*, 1992) have also been found to deviate from the standard Rossmann fold in distinctive manners.

In spite of the structural differences noted above for isocitrate dehydrogenase versus Rossmann-fold dehydrogenases, it should be noted that both classes of enzyme do in fact share certain features in the binding and conformation of NAD(P) as compared to the crystal structures of free NAD (Table III). All of the dehydrogenase ternary complexes solved to date show a uniform average distance of approximately 14–15 Å between the nucleotide rings, with an angle between the rings varying from 47° to 82°. Conversely, the crystal structure of NAD free acid shows the cofactor to adopt a folded conformation with the rings closer together and stacked nearly parallel to one another (distance 9.6 Å, angle 14°). The distance between rings of the unbound NAD^+ lithium salt is slightly longer, at 11.5 Å. Dehydrogenases such as lactate dehydrogenase and isocitrate dehydrogenase may exhibit an extension of the bound cofactor relative to its conformation in solution, with a concurrent twisting of the nucleotide rings away from a parallel stacked geometry in order to maximize binding interactions between protein and cofactor.

Inhibition by Calcium. The calcium ion is complexed by isocitrate, three conserved aspartate residues (307, 311, and 283′), and two water molecules (Figure 4) with bond distances and angles between the metal, the protein side chains, and the bound waters which are virtually the same as those observed for a number of crystal structures of calcium-binding proteins found in the Brookhaven Protein Data Bank (Bernstein *et al.*, 1977), including parvalbumin (Br ookhaven no. 5CPV; Moews & Kretsinger, 1975), intestinal calcium binding protein (31CB; Szebenyi *et al.*, 1981), calmodulin (3CLN; Babu *et al.*, 1988), and troponin C (5TNC; Herzberg & James, 1985). These proteins all exhibit bond distances ranging from 2.2 to 2.6 Å. In almost every case there is a bound water molecule associated with each metal ion. Highly refined crystal structures indicate that the coordination number of Ca^{2+} ion in most proteins is 7 (pentagonal bipyramidal) rather than 6 (octahedral) (Strynadka & James, 1989). This alternate coordination

assignment can also be accommodated by isocitrate dehydrogenase, depending on the assignment of ligand interactions between the metal ion and the isocitrate substrate oxygens.

In the wild-type enzyme, the bound magnesium ion may play a number of roles in catalysis, including orientation of the substrate molecule for deprotonation and subsequent formation of an enediolate, stabilization of an oxyanion transition state, and participation in acid–base catalysis through inductive effects on the pK_a of the side chain(s) which participate in dehydrogenation. Calcium ion apparently is almost incapable of performing a similar role in the enzyme active site. The distances between the calcium ion and the oxygens of isocitrate are longer than the Mg^{2+} complex (3.0 Å as compared to 2.4 Å). These abnormal distances between metal and substrate may result in the enzyme being unable to significantly reduce the energy of the transition state of the enolate complex which is presumed to form during isomerization. However, the individual binding of the metal ion and the substrate molecule by the enzyme active-site residues appears to be tight for both species, leading to the conclusion that the balance between metal binding and substrate binding in enzymatic turnover is delicate and prone to disruption by foreign metal species. This observation is confirmed by the results of many metal-substitution experiments in other enzyme systems, such as superoxide dismutase (Ose & Fridovich, 1979; Yamakura & Suzuki, 1980).

In addition to the long chelation distances between isocitrate and calcium, it is also possible that the interactions between isocitrate and the nicotinamide ring described here are also reflective of an unproductive ternary complex. Specifically, the close proximity of the lysine 230′ and tyrosine 160 to the β-carboxyl of isocitrate (interactions which are also observed in the binary complex of isocitrate and magnesium) should inhibit decarboxylation, and these hydrogen bonds must break upon formation of the full ternary complex in order for decarboxylation to occur. In addition, the salt bridge between the γ-carboxyl of isocitrate and the nicotinamide nitrogen might inhibit hydride transfer; in this case it is possible that an alternative mechanism of association between isocitrate and cofactor might be observed in the true Michaelis complex.

ACKNOWLEDGMENT

The authors would like to acknowledge the kinetic data which was provided by Dr. Myoung Lee and the kindness of Dr. Len Banaszak's laboratory members in providing XPLOR parameter and topology files for NAD.

REFERENCES

Adams, M. J., Ford, G. C., Koekok, R., Lentz, P. J., Jr., McPherson, A., Jr., Rossmann, M. G., Smiley, I. E., Schevitz, R. W., & Wonacott, A. J. (1970) *Nature 227*, 1098–1103.

Babu, Y. S., Bugg, C. E., & Cook, W. J. (1988) *J. Mol. Biol. 203*, 191–204.

Bernstein, F. C., Koetzle, T. F., Williams, G. J. B., Meyer, E. F., Jr., Brice, M. D., Rodgers, J. R., Kennard, O., Shimanouchi, T., & Tasumi, M. (1977) *J. Mol. Biol. 112*, 535–542.

Birktoft, J., Rhodes, G., & Banaszak, L. (1989) *Biochemistry 28*, 6065–6081.

Brunger, A. T., Kuriyan, J., & Karplus, M. (1987) *Science 235*, 458.

Dean, A. M., & Koshland, D. E., Jr. (1990) *Science 249*, 1044–1046.

Dean, A. M., & Koshland, D. E., Jr. (1993) *Biochemistry* (first of three papers in this issue).

Eklund, H., Samama, J., Wallen, L., Branden, C., Akeson, A., Jones, T. (1981) *J. Mol. Biol. 146*, 561–587.

Eklund, H., Samama, J., & Jones, T. (1984) *Biochemistry 23*, 5982.

Grau, U., Trommer, W., & Rossmann, M. (1981) *J. Mol. Biol. 151*, 289–307.

Gronenborn, A. M., Clore, G. M., and Jeffery, J. (1984) *J. Mol. Biol. 172*, 559–570.

Herzberg, O., & James, M. N. G. (1985) *Nature 313*, 653–659.

Hurley, J. H., Thorsness, P. E., Ramalingam, V., Helmers, N. H., Koshland, D. E., Jr., & Stroud, R. M., (1989) *Proc. Natl. Acad. Sci. U.S.A. 86*, 8635–8639.

Hurley, J. H., Dean, A. M., Sohl, J. L., Koshland, D. E., Jr., & Stroud, R. M. (1990a) *Science 249*, 1012–1016.

Hurley, J. H., Dean, A. M., Thorsness, P. E., Koshland, D. E., Jr., & Stroud, R. M. (1990b) *J. Biol. Chem. 265*, 3599.

Hurley, J. H., Dean, A. M., Koshland, D. E., Jr., & Stroud, R. M. (1991) *Biochemistry 30*, 8671–8678.

Jones, T. A. (1978) *J. Appl. Crystallog. 11*, 268–272.

Kim, J.-J. P., & Wu, Y. (1988) *Proc. Natl. Acad. Sci. U.S.A. 85*, 6677–6681.

Konnert, J. H., & Hendrickson, W. A. (1980) *Acta Crystallogr. A36*, 344–350.

Kornberg, H. L., & Madsen, N. B. (1957) *Biochim. Biophys. Acta 24*, 651–653.

LaPorte, D. C., & Koshland, D. E., Jr. (1982) *Nature 300*, 458–460.

LaPorte, D. C., Thorsness, P. E., & Koshland, D. E., Jr. (1985) *J. Biol. Chem. 260*, 10563–10568.

Moews, P. C., & Kretsinger, R. H. (1975) *J. Mol. Biol. 91*, 201–228.

Moras, D., Olsen, K., Sabesan, M., Buehner, M., Ford, G., & Rossmann, M. (1975) *J. Biol. Chem. 250* (23), 9137–9162.

Parthasarathy, R., & Fridey, S. (1984) *Science 219*, 969–971.

Ose, D. E., & Fridovich, I. (1979) *Arch. Biochem. Biophys. 194*, 360–364.

Reeves, H. C., Gaston, O. D., Chen, C. L., & Houston, M. (1972) *Biochim. Biophys. Acta 258*, 27–39.

Rondeau, J.-M., Tete-Favier, F., Podjarny, A., Reymann, J.-M., Barth, P., Biellmann, J.-F., & Moras, D. (1992) *Nature 355*, 469–472.

Strynadka, N. C. J., & James, M. N. G. (1989) *Annu. Rev. Biochem. 58*, 951–998.

Szebenyi, D. M. E., Obendorf, S. K., & Moffat, K. (1981) *Nature 294*, 327–332.

Thorsness, P. E., & Koshland, D. E., Jr. (1987) *J. Biol. Chem. 262*, 10422–10425.

Yamakura, F., & Suzuki, K. (1980) *J. Biochem. (Tokyo) 88*, 191–196.